Photophysical Study of 3-Acetyl-4-oxo-6,7-dihydro-12*H*-indolo[2,3-*a*]quinolizine in Biomimetic Reverse Micellar Nanocavities: A Spectroscopic Approach

Arabinda Mallick,[†] Basudeb Haldar,[†] Subhendu Maiti,[‡] Subhash Chandra Bera,[†] and Nitin Chattopadhyay*,[†]

Department of Chemistry, Jadavpur University, Calcutta 700 032, India, and Department of Chemistry, Jalpaiguri Government Engineering College, Jalpaiguri 735 102, India

Received: January 29, 2005; In Final Form: May 27, 2005

Photophysical properties of 3-acetyl-4-oxo-6,7-dihydro-12*H*-indolo[2,3-*a*]quinolizine (AODIQ), a bioactive molecule, has been investigated in well-characterized, monodispersed biomimicking nanocavities formed by sodium bis(2-ethylhexyl)sulfosuccinate (AOT) in heptane using steady-state and picosecond time resolved fluorescence and fluorescence anisotropy. The emission behavior of AODIQ is very much dependent upon the water/surfactant mole ratio (*W*), i.e., on the water pool size of the reverse micellar core. AODIQ exhibits a sharp decrease in fluorescence anisotropy with increasing *W*, implying that the overall motional restriction experienced by the molecule is decreased with increased hydration. Some of the depth-dependent relevant fluorescence parameters, namely, fluorescence maxima and fluorescence anisotropy (*r*), have been monitored for exploiting the distribution and microenvironment around the probe in the reverse micelles. Fluorescence spectral position and fluorescence quenching studies suggest that the probe does not penetrate into the reverse micellar core; rather it binds at the interfacial region. Quantitaive estimates of the micropolarity and microviscosity at the binding sites of the probe molecule have been determined as a function of *W*.

Introduction

In the past 2 decades, the importance of organized assemblies on biological and photophysical processes has been recognized. Reactants accommodated in molecular assemblies such as micelles, microemulsions, and vesicles, etc., often achieve a greater degree of organization compared to their geometries in homogeneous solution, can mimic reactions in biosystems, and also have potential for energy storage.[1] The behavior of an organic molecule at an interface between two bulk media is often significantly different from that in either of the bulk media. Since the polarity and viscosity at the interface are often very much different from those of the bulk media, the structure, dynamics, and reactivity of an organic or biomolecule at an interface differ markedly from those observed in the bulk. Interestingly most natural and biological processes occur at such interfaces or in confined systems, e.g., proteins, biomembranes, and vesicles. The wide range of function performed by biological membranes and membrane proteins have motivated the researchers to look for simple model systems, which can mimic, at least in part, the physicochemical properties of the membrane architecture. Typical examples of such membrane mimetic models are "micelles" and "reverse micelles", which are organized assemblies of surfactants in aqueous and organic solvent media, respectively.[2,3] Reverse micelles, in particular, afford the opportunity of examining molecules with various states of hydration, Luisi investigated and simulated situations present in water-restricted environments prevailing the self-reproduction in supramolecular systems.[4] Such model systems are able to capture a number of essential features of biological membranes though lacking much of their complexities. It has also been reported that enzyme containing reverse micelle may offer novel tools for biotechnology and for drug delivery through solubilization of liophilic drugs.[5,6] The popularity of reverse micelles for model enzyme catalysis stems from the fact that the micellar core is capable of binding and orienting substrates that can be very specific to certain functionalities as much as enzymes would do. Works in the area of micellar and reverse micellar environments are of growing importance and are recognized as tools for better understanding of chemistry and the mechanistic aspect of reactions and as a route to improve yields of reactions.[7] It is well-known that the dynamics of liquids in confined spaces is different from that of their bulk counterparts[8] and thus constitutes one of the main reasons for the popularity that reverse micelles enjoy as a model system in studies of water dynamics. In particular, reverse AOT (bis(2-ethylhexyl)sulfosuccinate) micelles have been studied extensively during the past decades.[9,10] It is a nontoxic compound and can be used in pharmaceutical and medicinal preparations. Unlike most amphiphiles and like many phospholipids, it is a double-tailed anionic surfactant which can be conveniently used for solubilization and emulsification purposes. As one of the several advantages of a reverse AOT micellar system, the size of the water pool can be controlled precisely at the nanometer level through the molar ratio of water/surfactant. Therefore size effect on chemical and physical properties in nanometer dimensions can be studied by the use of AOT micelles. In heptane the radius (r_w) of such a water pool is about 2*W* (in angstroms), where *W* is the number of water to the surfactant molecules.[11,12] Through modern studies it is revealed that there are three types of water molecules in the water pool, at the peripheries of the pool one strongly held by the polar or ionic headgroups of the surfactants and are thus "bound", the "trapped" water is between the surfactant while that at the center of the pool, in all respects, is similar to the interfacial water

* Corresponding author. E-mail: pcnitin@yahoo.com.
† Jadavpur University.
‡ Jalpaiguri Government Engineering College.

10.1021/jp050511d CCC: $30.25
Published on Web 07/07/2005

CHART 1: Structure of AODIQ

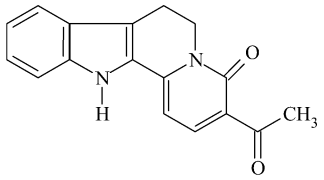

present near biological membranes or protein surfaces and is relatively "free".[12] Jain et al.[13] established the presence of three types of water molecules in reverse micelles using FTIR spectroscopy. The amount of bound and free water molecules present in such a microemulsion has been estimated by many workers.[12,13] However, a more recent model envisages an equilibrium between the bound and free water in biological systems which result in the bimodal dielectric relaxation.[14] The bulk properties such as the polarity and viscosity of the free and bound water vary with a change in the *W* value in the reverse micellar situation.[15−17]

A fluorescent molecular probe plays an important role in demonstrating as well as characterizing the microenvironment.[18,19] The fluorophore, 3-acetyl-4-oxo-6,7-dihydro-12*H*-indolo[2,3-*a*]quinolizine (AODIQ), a neutral molecule, used in the present experiment has recently been shown to be an excellent fluorescent probe for biological systems[20,21] and belongs to the bioactive indole family. It is well-known that reactive oxygen species (ROS) participate in a number of pathological processes in the nervous system. Compounds able to interfere with the action of ROS might be useful in prevention and treatment in these pathologies. Recently attention has been focused toward designing and synthesizing compounds with a suitable spectrum of pharmacological and pharmacokinetic properties, among which indole derivatives are distinct groups with great potential. The indole nucleus seems to be a promising basis for designing and synthesizing new derivatives able to protect the nervous system.[22] Molecules containing an indole nucleus such as β-carbolines and carbazoles are, by now, well-established as bioactive molecules.[23−27] The single-step synthesis of AODIQ from 1-methyl-3,4-dihydro-β-carboline[28] also leads to the presumption that the molecule should have biological activity**.** The spectroscopic and photophysical data of this molecular system in homogeneous and microheterogeneous media are very useful for a better understanding of the biodistribution of this dye inside the living cell. The basic intention of the present spectroscopic research on AODIQ is to explore the potential usefulness of its fluorescence properties for understanding its interaction with relevant biological targets such as proteinsn and membranes, etc. In our continuing effort we have already studied the interaction of this molecular system in micellar and proteinous environments.[20,21] From the viewpoint of future biophysical applications, it seems interesting to make a vivid study of the photophysical processes of AODIQ in AOT reverse micelle.

Experimental Section

AODIQ (Chart 1) was synthesized in the laboratory using the method mentioned elsewhere.[28] It was purified by column chromatography, and the purity of the compound was checked by thin-layer chromatography (TLC). Further the compound was vacuum-sublimed before use. Triply distilled water was used for making the experimental solutions. Purification and drying of AOT (Aldrich) is described elsewhere.[13,29] The concentrated stock solution of AODIQ was prepared in 1,4-dioxane, and a fixed amount of this concentrated solution was added to each experimental solution. The solutions were prepared using the literature procedure[18] but in a reverse way; i.e., the surfactant concentration was varied instead of the water concentration.

The absorption and steady-state fluorescence measurements were performed using a Shimadzu MPS 2000 spectrophotometer and a Spex Fluorolog II spectrofluorimeter, respectively. The steady-state fluorescence anisotropy was performed with a Hitachi spectrofluorimeter F-4010 model. Excitation and emission bandwidths were 5 nm. Steady-state anisotropy, *r*, was defined by

$$r = (I_{VV} - GI_{VH})/(I_{VV} + 2GI_{VH})$$

where I_{VV} and I_{VH} are the intensities obtained with the excitation polarizer oriented vertically and the emission polarizer oriented vertically and horizontally, respectively. The *G* factor was defined as

$$G = I_{HV}/I_{HH}$$

I terms refer to parameters similar to those mentioned above for the horizontal position of the excitation polarizer. Quantum yields were determined using quinine sulfate in 0.1 N H_2SO_4 ($\varphi_f = 0.54$).[30] Fluorescence lifetimes were determined from time-resolved intensity decay by the method of time-correlated single-photon counting using a picosecond diode laser at 408 nm (IBH, U.K., nanoLED-07) as the light source. The typical response of this laser system was 70 ps. The decays were analyzed using IBH DAS-6 decay analysis software. The same software was also used for anisotropy analysis. For all the lifetime measurements the fluorescence decay curves were analyzed by the biexponential iterative fitting program provided by IBH. Mean (average) fluorescence lifetime (τ) for biexponential iterative fitting were calculated from the decay times and the preexponential factors using the following relation:

$$\langle\tau\rangle = a_1\tau_1 + a_2\tau_2 \qquad \text{(i)}$$

Results and Discussion

In *n*-heptane, AODIQ exhibits an emission band with a clear vibrational structure (see Figure 1 of ref 31). In AOT (0.1 M) the vibrational pattern still persists, although the structural nature is much blurred compared to that observed in the spectrum of AODIQ in nonpolar solvents. As we move from $W = 0$ to higher water contents, the vibrational band disappears gradually. This observation suggests that the probe molecule is gradually incorporated toward the more polar region. A remarkably less structured emission in AOT/*n*-heptane medium is indicative of the fact that there is always some water of hydration even with the dried AOT.

Figure 1 depicts the emission spectra of AODIQ in AOT reverse micelles at different values of *W*.

In a recent work[31] we have reported that AODIQ has dual emission, one locally excited (LE) and the other charge transfer (CT), depending upon the polarity of the medium; the former predominantly existing in less polar and the latter in highly polar environments. The quantum yield of AODIQ fluorescence is known to depend on the polarity of the medium in which the probe is located, and it forms a bell-shaped curve; i.e., with an increase in solvent polarity, φ attains a maximum and then decreases again (vide supra, inset of Figure 8). In the present case from the initial addition of water ($W = 2$) AODIQ shows strong CT emission. As we go from $W = 0$ to higher *W* values, the emission maximum goes toward red (inset of Figure 1) along with a small increase in the fluorescence yield. Both observa-

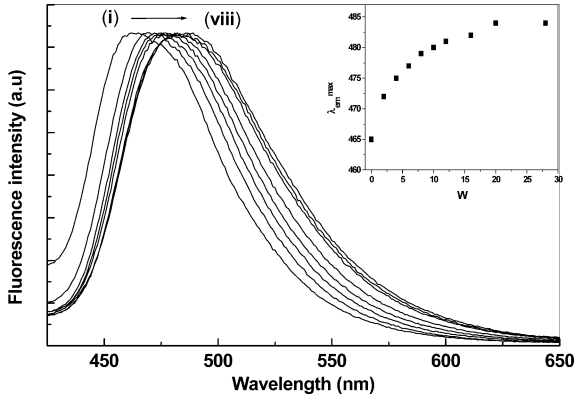

Figure 1. Normalized fluorescence spectra of AODIQ in AOT/*n*-heptane reverse micelles as a function of W ($\lambda_{exc} = 420$ nm). Curves i → viii correspond to $W = 0$, 2, 4, 6, 10, 16, 20, and 28, respectively. The inset shows the variation of fluorescence maximum as a function of W.

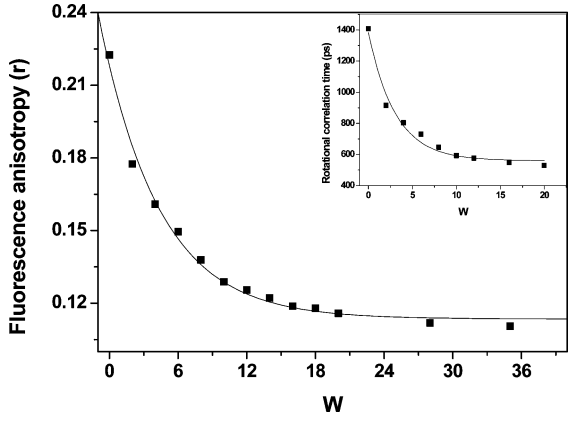

Figure 2. Variation of fluorescence anisotropy (r) of AODIQ in AOT/*n*-heptane reverse micelles as a function of W. The inset shows the variation of rotational correlation time as a function of W.

tions reflect that the microenvironment around the probe gets modified as we move from lower W to higher W. In such a microemulsion of $W = 28$ AODIQ exhibits intense emission with emission maximum at 485 nm. The emission maximum of AODIQ in the reverse micelle is about 35 nm, blue shifted from that of AODIQ in water (520 nm). Such a dramatic difference of emission maximum in the reverse micellar environments compared to that of bulk water indicates that the microenvironment of AODIQ is significantly different from the bulk water. As more and more water is added, the water pool swells in size and the polarity of the microenvironment increases,[32,33] resulting in the red shift in the emission maximum. The observed shift denotes an important point, that the change in polarity experienced in anisotropic assemblies will be dependent on the position (location) of the probe molecule. Kelker et al.[34] explained this issue using anthroloxy probes of different chain length and showed that the shift in the emission maximum decreases as the distance of the fluorophore increases from the water pool. Using 7-nitrobenz-2-oxa-1,3-diazol-4-yl (NBD)−cholesterol, they found that the emission maximum was invariant with increased W number, indicating that the probe molecule is located in a region far from the water pool of the reverse micelle. In the present investigation, the emission maximum is sensitive to W up to a certain level; the emission maximum still remaining 35 nm blue-shifted from that in the bulk water. Following the work of Hazra et al. and Kelker et al.[8,34] from the dependence of the shift of the emission maximum on W, we rule out the possibility of localization of the probe molecule in a region far from the reverse micellar core (bulk heptane). A remarkable difference in the position of the emission maximum in reverse micelles and bulk water suggests that the probe molecule does not reside (or only a part of it resides) at the core region. Apart from the bathochromic shift in the reverse micelles, the fluorescence spectra show a remarkable change in fluorescence yield accompanied by a spectral broadening. The emission yield of the CT band increases appreciably. This can be rationalized in terms of localization of the probe in a more polar (hydrated) site, i.e., toward the core of the reverse micelles. Spectral broadening may be due to increased heterogeneity of AODIQ solvation with increased hydration of the reverse micelles, a situation encountered when the rate of the solvent reorientation in the excited state is comparable to the fluorescence lifetime.[35]

Steady-State Fluorescence Anisotropy Study. Measurement of fluorescence anisotropy has a demanding role for its tremendous potential in biochemical research because any factor that affects size, shape, or segmental flexibility of a molecule will affect the observed anisotropy.[34] Keeping in mind the wide application of fluorescence anisotropy in the studies of biochemical/biophysical interest, steady-state fluorescence anisotropy has been performed in the present work. Fluorescence anisotropy reflects the extent of restriction imposed by the microenvironment on the dynamic properties of the probe; thus it can be exploited for finding out the probable location of the probe in the reverse micellar environments. Figure 2 represents the variation of fluorescence anisotropy (r) of AODIQ in AOT/heptane as a function of water pool size W.

It is evident from Figure 2 that fluorescence anisotropy decreases as W increases, which suggests that the probe molecule experiences a considerable freedom in motion with an increase in the W value. Figure 2 reflects that r decreases rapidly until $W = 15$ and then levels off gradually. Similar results have been reported by Sengupta et al.[17,18] It has been established that water relaxation rates in reverse micelles become faster with an increase in W.[37] This increase in reorientation rate is reflected in the reduced anisotropy for probes in reverse micellar interface and water pool.[39] At the highest W we have examined, ($W = 28$) the observed anisotropy ($r = 0.11$) is still higher than the anisotropy in pure water ($r = 0.04$), indicating that the probe molecule in the reverse micelle still experiences reasonable restriction compared to the situation in bulk water. This suggests that the AODIQ molecule is probably located at the water/surfactant interface of AOT reverse micelles.

Micropolarity around the Fluorophore. Due to the great importance of the determination of microscopic polarity of biological systems using fluorescent probes,[40−42] attention has been drawn for the past few decades to this direction. In an earlier study[31] it was observed that the fluorometric behavior of AODIQ is very much dependent on the solvent polarity. Taking advantage of this polarity-sensitive fluorescence property of AODIQ, we studied the polarity of the microenvironment in micelles and proteins.[20,21] However very few reports have appeared so far on the prospective use of fluorescence characteristics of such a polarity-sensitive fluorescent molecule for the determination of micropolarity in membrane mimetic models and reverse micelles. The micropolarity of a biological system like protein, membrane, and reverse micelles can be estimated by comparison of the spectral properties of a fluorophore in that environment with those of the probe in solvents of known polarity.[20,21,25,40,43−45] To get a quantitative measure of the polarity of the local environment of AODIQ in reverse micelles, the empirical solvent polarity parameter, $E_T(30)$, based on the transition energy for the solvatochromic intramolecular charge-

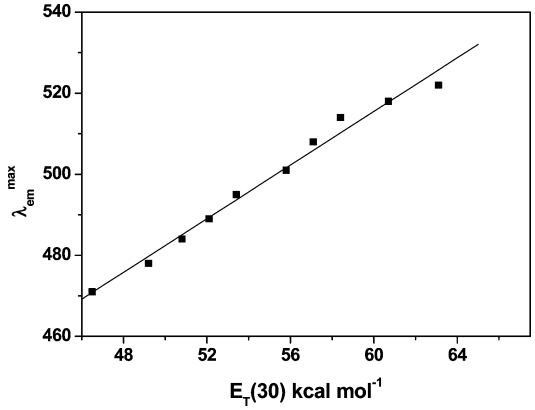

Figure 3. Variation of emission maximum of AODIQ in the dioxane−water mixture.

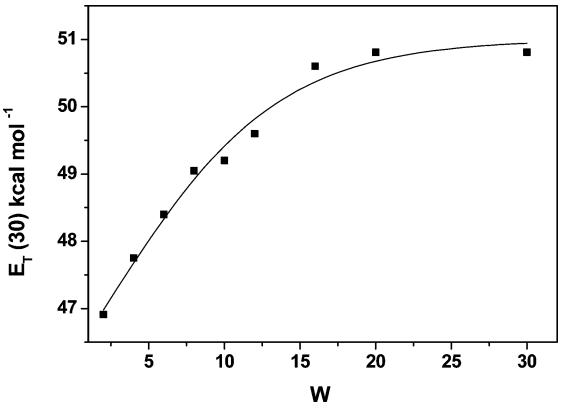

Figure 4. Plot of $E_T(30)$ against W of AODIQ in AOT/*n*-heptane reverse micelles.

transfer absorption of the betaine dye 2,6-diphenyl-4-(2,4,6 triphenyl-1-pyridono)phenolate as developed by Reichardt, has been used.[46,47] For this purpose, we have studied the fluorescence behavior of AODIQ in water−dioxane mixtures of varying composition.[31] A representative plot monitoring the CT fluorescence maximum of AODIQ in a water−dioxane mixture against $E_T(30)$ establishes a linear correlation between the two (Figure 3).

From the position of the CT maximum of AODIQ at different W, we have determined, in terms of $E_T(30)$, the micropolarity around the probe in reverse micelles with various W values. The variation of micropolarity of AODIQ in reverse micellar environments as a function of W has been represented in Figure 4.

Figure 4 clearly shows that, with increasing W, $E_T(30)$ increases rapidly until $W = 15$ and levels off beyond that. At the highest W we have examined ($W = 28$), the $E_T(30)$ value is 50.8, indicating that the average environment of the probe molecules is still less polar than that of bulk, water which further supports our earlier prediction from anisotropy study that the probe resides at the water−surfactant interface.

Microviscosity around the Fluorophore. Fluorescence anisotropy is very much dependent upon the viscosity of the environment around the fluorophore. Thus, microviscosity, at a fixed temperature, is often estimated by comparing the fluorescence anisotropy of a fluorophore in an environment with those of the probe in solvents of known viscosities.[36,48] To get the variation of viscosity as a function of W in the reverse micellar environments, we followed the method as described separately by our group[20] and also by Wang et al.[48] in micellar environments. According to this method, r of AODIQ at

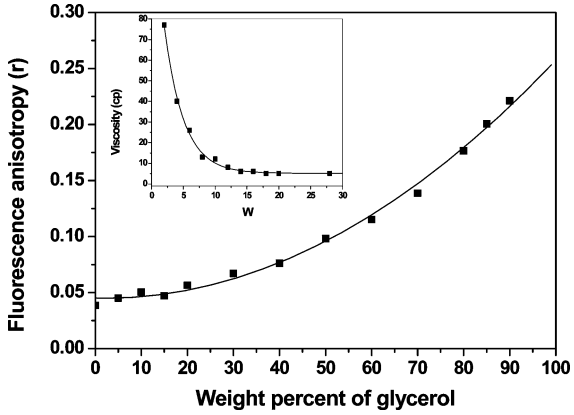

Figure 5. Variation of fluorescence anisotropy as a function of composition of the glycerol−water mixture. Inset shows the variation of microviscosity of AODIQ in AOT/*n*-heptane reverse micelles as a function of W.

TABLE 1: Photophyical Data of AODIQ as a Function of W^a

W	r_w (Å)	emission max (nm)	$E_T(30)$ (kcal mol^{-1})	r	η (cP)
0	0	465		0.222	
2	4	472	46.91	0.177	77
4	8	475	47.75	0.161	40
6	12	477	48.40	0.150	26
8	16	479	49.05	0.137	13
10	20	480	49.20	0.129	12
12	24	481	49.60	0.125	8
16	32	482	50.60	0.119	6
20	40	484	50.81	0.116	5
28	56	484	50.81	0.111	5
water		520	63.10	0.040	0.89

[a] W = [water]/[surfactant]; r_w = core size; $E_T(30)$ = micropolarity; r = steady-state fluorescence anisotropy; η = microviscosity.

different W were compared with the values in glycerol−water mixtures of different compositions at 298 K.[20,48,49] The calibration curve monitoring the fluorescence anisotropy of AODIQ in glycerol−water mixtures against the weight percentage composition of glycerol is presented in Figure 5.

By comparing the calibration curve based on the available data,[50] we have determined the microviscosity (error, 15%) in the reverse micelles of different W, and the variation is presented in the inset of Figure 5. The inset shows that as W increases, the microviscosity rapidly decreases until $W = 15$ and gradually decreases until the solution becomes turbid above $W = 28$ because of the limit of the water solubilization. The considerably high viscosity at low W is expected to be attributable to water molecules tightly bound to the sulfonate headgroup of AOT. In addition the inset of Figure 5 shows that the microviscosity at the vicinity of water/surfactant interface is considerably higher than that of bulk water even in a fully expanded state (microemulsion). Table 1 summarizes all the results obtained in steady-state analysis as a function of core size (W).

The properties of water in reverse micelles of AOT at different W are rather different from those of bulk water.[13] Literature suggests that even at high water content the apparent viscosity is 6−9 times greater than that of free water molecules.[51] Our estimated microviscosity at the highest W is very much close to the range of the earlier report.[51] Thus, the results led to the conclusion that AODIQ probe is useful for rapid determination of the microviscosity of AOT reverse micelles (particularly near the interfacial region) of different dimensions.

Metal-Induced Fluorescence Quenching Study. Quenching of fluorescence of AODIQ due to external heavy metal atom

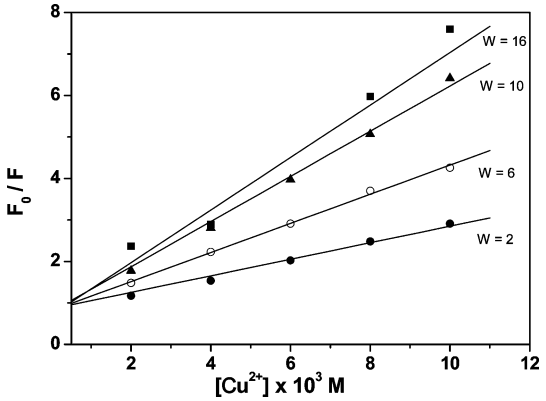

Figure 6. Variation of relative fluorescence intensity (F_0/F) of AODIQ in AOT/ *n*-heptane reverse micelles as a function of *W*.

has been studied as a function of *W* using ionic quencher Cu^{2+} with an intention to see how the accessibility of the probe molecule to the quencher depends on *W* and hence to throw some light on the probable location of the probe in the reverse micellar environment.

The results of these experiments for quenching of AODIQ by Cu^{2+} at different *W* are plotted in Figure 6 as Stern−Volmer plots.

The slope of such a plot (K_{SV}) is related to the degree of exposure (accessibility) of the probe to aqueous phase. In general, the higher the slope, the greater the degree of exposure.[36,52] It is apparent from Figure 6 that, with an increase in the *W* value, accessibility of AODIQ molecule to Cu^{2+} increases.

Figure 6 reveals that the quenching process becomes more favored as the *W* value (water pool size) increases. The efficiency of the quenching process is decreased with decreasing fluidity of the medium, which slows the rate of diffusion of the interacting species, consequently reducing the photophysical process. The quenching of fluorescence of different fluorophores by Cu^{2+} ion has been studied by Panda et al.[53] in aqueous and oil/water (o/w) microemulsion. The relatively low value of K_{SV} in microemulsion than that in aqueous medium was interpreted by the authors in terms of interfacial barrier (by way of solvation and separation) for interaction of fluorophore and quencher populated preferentially in the oil and water, respectively. It is imperative from the above account that the interfacial barrier and regional fluidity have a say on the photophysical process involving the fluorophore and the quencher. In the present investigation, most likely the probe is located in the interfacial region and the quencher resides in the interior of the water pool of the reverse micelles, so that the interaction propensity is essentially guided by both the interfacial barrier and fluidity of water inside the reverse micelle. At low *W*, the solvation of interfacially adsorbed AOT molecules in the water pool (to the extent of 1:6 as AOT:water)[54] fairly decreased the pool fluidity and hence reduced K_{SV}. Our result indicates that increasing *W* enhances the polarity of the microenvironment and induces increased hydration; i.e., movement of probe molecule toward the core region occurs with increasing *W*, resulting in a concomitant increase in the K_{SV}. This is also supported by the result of our anisotropy experiment where it is argued that the probe molecule gets relatively free in its motion as the core size increases, which in turn enhances the rate of diffusion of the interacting species and helps it to come closer to the quencher molecules. Although the relative order of K_{sv} values with a variation of *W* is meaningful, the absolute values should not be emphasized. Binding of the Cu^{2+} ions with the AOT

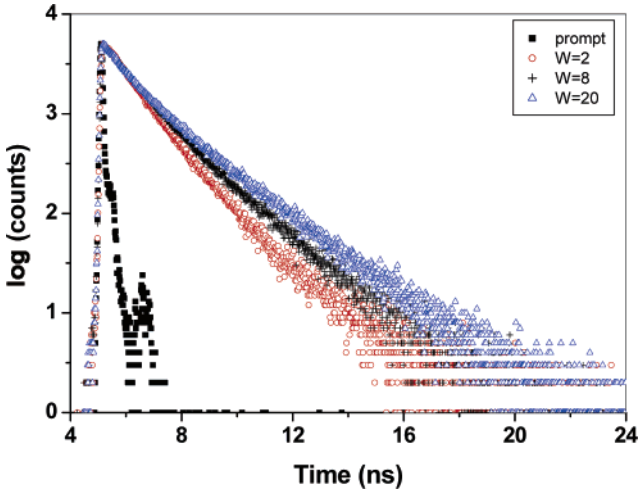

Figure 7. Time-resolved fluorescence intensity decay of AODIQ in AOT/*n*-heptane reverse micelles in different *W* (λ_{exc} = 408 nm). Inset shows the respective *W* values. The sharp profile on the left is the lamp profile.

reverse micelles[55] is expected to increase the local concentration of the quencher around the fluorophore bound to the interfacial region within the reverse micelle, leading to an increase in the K_{sv} values.

Time-Resolved Studies

Fluorescence lifetime serves as a sensitive parameter for exploring the local environment around a fluorophore,[56,57] and it is sensitive to excited-state interactions. Differential extents of solvent relaxations around a fluorophore could also be expected to give rise to differences in its lifetime. In reverse micelles, the decay of AODIQ becomes multiexponential and the lifetime values are observed to be longer than in pure aqueous solution. Obviously extraction of meaningful rate constants in such heterogeneous systems is really difficult. Robinson et al.[12] pointed out that if the diffusion coefficient (*D*) of the probe in the water pool is the same as that of an aromatic molecule in ordinary water (0.05Å^2 ps^{-1}), the probe molecule moves about 10 Å/ns in a direction normal to the surface ($Z^2 = 2D\langle t\rangle$). Thus, the AODIQ molecules pass through several water layers within the observed lifetime of ∼1 ns. Evidently the multiexponential decay originates from the different polarity regions experienced by the molecule within its lifetime. If the diffusion coefficient inside the water pool is smaller by 1 order of magnitude compared to that of pure aqueous medium, every AODIQ molecule would be more or less confined to one layer of water molecules. However, even then there is the possibility of different AODIQ molecules in different polarity regions being excited simultaneously. That superposition of many decays of slightly different lifetimes looks such as a biexponential decay is discussed by many workers.[12,58] Typical biexponential decay profiles of AODIQ in AOT reverse micelles of different *W* values are shown in Figure 7.

The fluorescence lifetimes of AODIQ in AOT reverse micelles obtained as a function of *W* are shown in Table 2.

Instead of placing too much emphasis on the magnitude of individual decay constants in such biexponential decays, we chose to use the mean fluorescence lifetime defined by eq i as an important parameter for exploiting the behavior of AODIQ molecule bound to AOT reverse micelles. The average lifetime values are given in Table 3. The most interesting feature of this investigation, in the case of this ICT probe, is the increase in the mean fluorescence lifetime with increased water content

TABLE 2: Lifetimes of AODIQ in AOT Reverse Micelles as a Function of W^a

W	a_1	τ_1 (ps)	a_2	τ_2 (ps)	χ^2
0	0.570	720	0.431	1378	1.15
2	0.572	744	0.428	1453	1.19
4	0.534	699	0.466	1544	1.24
6	0.537	674	0.463	1642	1.26
8	0.525	648	0.475	1698	1.24
10	0.520	626	0.480	1723	1.15
12	0.528	622	0.472	1800	1.31
16	0.525	591	0.475	1880	1.26
20	0.535	559	0.467	1946	1.19
water	0.808	671	0.193	1433	1.36

[a] W = [water]/[surfactant].

TABLE 3: Radiative and Nonradiative Rate Constants of AODIQ in AOT Reverse Micelles as a Function of W^a

W	φ_f	$\langle\tau_f\rangle$ (ps)	$k_r \times 10^{-12}$ (s^{-1})	$k_{nr} \times 10^{-12}$ (s^{-1})
0	0.162	1003	162	835
2	0.195	1047	186	769
4	0.197	1093	180	735
6	0.200	1122	178	713
8	0.197	1146	172	700
10	0.196	1152	170	698
12	0.202	1178	172	677
16	0.203	1203	170	662
20	0.203	1207	168	662
water	0.080	817	0.098	1125

[a] W = [water]/[surfactant]; φ_f at $W = 28$ was measured to be 0.196.

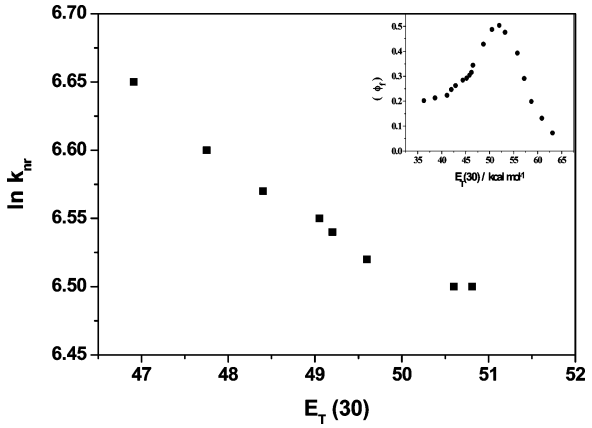

Figure 8. Plot of ln k_{nr} vs $E_T(30)$ in the reverse micellar solutions. Inset shows the variation of fluorescence quantum yield (φ_f) as a function of solvent polarity $E_T(30)$ for water−dioxane mixtures with varying compositions.

in the micelle. Thus, the mean fluorescence lifetime increases from ≈1000 to ≈1200 ps when the [water]/[surfactant] mole ratio is changed from 0 to 20, which is in sharp contrast with the experiments of Chattopadhyay et al., Datta et al., and Chattopadhyay et al. using different ICT/TICT probes.[11,59−61] The above results are well-consistent with our previous observations[31] in which it was reported that the fluorescence yield of the CT state of AODIQ initially increases up to $E_T(30) \approx 52$ and then decreases again; i.e., the fluorescence quantum yield of AODIQ makes a bell-like pattern against the solvent polarity (see inset of Figure 8). In very low polar solvent like dioxane or heptane AODIQ does not exhibit any ICT emission, obviously because at such low polarity the barrier for formation of ICT from the LE state is too high to be surmounted. As the polarity of the medium increases, the yield of the ICT emission increases to a $E_T(30)$ value of ≈52 and the yield gradually decreases with further increase in the polarity. To explain this, it was considered that there are two competing processes—formation of the ICT state and subsequent nonradiative decay of the ICT state. The rate of formation of the ICT state increases with solvent polarity. Again with the increasing solvation of the ICT state the energy gap between the ICT state and low-lying triplet and/or ground state decreases. According to the energy gap law of nonradiative transitions, a decrease in the energy gap results in an increase in the nonradiative rates and hence decreasing the yield of the ICT state. As a matter of fact this kind of rise and fall is a very general phenomenon.[47,62−65] Although the competition between the two processes seems to explain the phenomenon qualitatively, but no quantitative explanation is available right now. It may be mentioned that Eisenthal and co-workers have proposed an empirical relation between the formation rate of TICT and $E_T(30)$ values.[66,67] However, no such relationship, empirical or otherwise, between the nonradiative transitions of the ICT processes and the polarity parameter is known. In pure water, AODIQ lifetime reduces to ≈817 ps, which has been attributed to the stabilized CT state, which is accompanied by an increase in the nonradiative decay (see Table 3). From the observed φ_f and τ_f, we can calculate the radiative and nonradiative rate constants for the ICT processes using the following relations (ii) and (iii), which is more important in supporting and for explaining the above observation.

$$k_r = \varphi_f/\tau_f \quad \text{(ii)}$$

$$1/\tau_f = k_r + k_{nr} \quad \text{(iii)}$$

where φ_f, τ_f, k_r, and k_{nr} are the fluorescence quantum yield, mean fluorescence lifetime, radiative rate constant, and nonradiative rate constants, respectively. All the photophysical parameters are tabulated in Table 3.

It is apparent from the above table that in reverse micelles nonradiative rate constant k_{nr} is gradually decreasing as W increases. The plot of ln k_{nr} against $E_T(30)$ (Figure 8) also bears a linear relationship but with negative slope up to a certain polarity, then attains a plateau, and then again increases (see the data for water) which is in tune with our earlier observations[31] in the case of variation of fluorescence quantum yield with solvent polarity (see the inset of Figure 8).

We have also compared the nonradiative rate-constant of the ICT process in reverse micelles to that in pure water. The k_{nr} in water is remarkably higher than in the reverse micelles. The nonradiative rate constant for ICT process in different reverse micelles is dependent substantially on the location of the probe.[8] From the variation of emission spectra with increased hydration, the localization in far *n*-heptane region was ruled out. Again, from the differences in the steady-state fluorescence, anisotropy, fluorescence lifetime, and nonradiative rate constant of the probe in the reverse micellar system from the corresponding parameters in the bulk water, it is reasonable to rule out the possibility of localization of the probe in the core region. Furthermore, since the probe molecule is neutral, it is very logical to assume that the probe molecule resides at the micelle−water interface. In this connection it is pertinent to mention at this point that in the case of micellar environments with different surface charges, we have shown that the probe molecule was located at the micelle−water interfacial region irrespective of the surface charges.[20]

Fluorescence anisotropy is a property which is dependent upon rotational diffusion of the fluorophore and the fluorescence lifetime. To ensure that the observed change in steady-state anisotropy of AODIQ as a function of W is not due to any change in lifetime, the apparent (average) rotational correlation times for AODIQ in AOT reverse micelles with increasing

hydration were calculated using Perrin's equation.[36]

$$\tau_c = (\langle\tau_f\rangle r)/(r_0 - r) \qquad \text{(iv)}$$

where r_0, r, and $\langle\tau_f\rangle$ are the limiting anisotropy, steady-state anisotropy, and mean fluorescence lifetime of AODIQ, respectively. Although the Perrin's equation is not strictly valid in heterogeneous media, using the mean fluorescence lifetime we can approximately apply the equation to the present case. Using eq iv, we have determined the rotational correlation times with varying W taking $r_0 = 0.37$ (determined from time-resolved anisotropy study, not shown here). The variation of rotational correlation time against W is represented in the inset of Figure 2. From the figure it is clear that there is a significant decrease in the rotational correlation time which clearly shows that the observed change in anisotropy values (Figure 2) were not due to lifetime-induced phenomena and reinforces our earlier prediction that there is a decrease in the rotational restriction experienced by the probe molecules with increasing hydration.

Conclusion

The present investigation reports the study of interactions of a newer, polarity sensitive biologically active fluorophore, showing efficiency in characterizing the reverse micellar microenvironments. The photophysical behavior of AODIQ is dramatically modified in reverse micelles from that of the bulk aqueous phase. This has been exploited to determine the nature of the microenvironment around the probe, and finally the micropolarity as well as microviscosity at the binding site as a function of reverse micellar core size (W). The study further suggests the probable location of the probe in the reverse micellar microenvironment. Extension of the present work in different complex and microheterogeneous environments such as proteins and allied enzymes should have a significant impact from a biological point of view in terms of understanding the environments in detail.

Acknowledgment. Financial support from CSIR and DST, Government of India, is gratefully acknowledged. B.H. is thankful to the CSIR for a research fellowship. The authors appreciate the cooperation received from Professor S. Basak and H. Chakraborty of SINP and Dr. N. Sarkar and A. Chakraborty of IIT Kharagpur for their kind help in steady state fluorescence anisotropy and time-resolved measurements, respectively.

References and Notes

(1) Hashimoto, S.; Thomas, J. K. *J. Am. Chem. Soc*. **1985**, *107*, 4655.
(2) Luisi, P. L.; Magid, L. J. *CRC Crit. Rev. Biochem*. **1986**, *20*, 409.
(3) Luisi, P. L.; Giomini, M.; Pileni, M. P.; Robinson, B. H. *Biochim. Biophys. Acta* **1988**, *947*, 209.
(4) Luisi, P. L. *Adv. Chem. Phys.* **1996**, *92*, 425.
(5) Luisi, P. L., Straube, B. E., Eds.; *Reverse Micelles*; Plenum Press: New York, 1984.
(6) Chang, G. G.; Hung, T. M.; Hung, H. C. *Proc. Natl. Sci. Counc., Repub. China, Part B: Life Sci.* **2000**, *24*, 89.
(7) Moulik, S. P.; Mukherjee, K. *Proc. Indian Natl. Sci. Acad., Part A* **1996**, *62*, 215.
(8) Hazra, P.; Chakraborty, D.; Sarkar, N. *Langmuir* **2002**, *18*, 7872.
(9) Riter, R. E.; Willard, D. M.; Levinger, N. E. *J. Phys. Chem. B* **1998**, *102*, 2705.
(10) Politi, M. J.; Chaimouich, H. *J. Phys. Chem*. **1986**, *90*, 282.
(11) Mandal, D.; Pal, S. K.; Datta, A.; Bhattacharya, K. *Anal. Sci*. **1998**, *14*, 199.
(12) Cho, C. H.; Chung, M.; Lee, J.; Nguyen, T.; Singh, S.; Vedamulthu, M.; Yao, S.; Zhu, S. B.; Robinson, G. W. *J. Phys. Chem*. **1995**, *99*, 7806.
(13) Jain, T. K.; Varshey, M.; Maitra, A. *J. Phys. Chem*. **1989**, *93*, 7409.
(14) Bagchi, B.; Chandra, A. *Adv. Chem. Phys*. **1990**, *80*, 1.
(15) Pileni, M. P., Ed. *Structure and Reactivity in Reverse Micelles*; Elsevier: Amsterdam, 1981.
(16) Robinson, G. W.; Chu, S. B.; Singh, S.; Evans, M. W. *Water in Biology, Chemistry and Physics*; World Scientific: Singapore, 1996.
(17) Sengupta, B.; Sengupta, P. K. *Spectrochim. Acta, Part A* **2000**, *56*, 1433.
(18) Guharay, J.; Sengupta, P. K. *Biochem. Biophys. Res. Commun*. **1996**, *219*, 388.
(19) Mallick, A.; Chattopadhyay, N. *Biophys. Chem*. **2004**, *109*, 261.
(20) Mallick, A.; Haldar, B.; Maiti, S.; Chattopadhyay, N. *J. Colloid. Interface Sci*. **2004**, *278*, 215.
(21) Mallick, A.; Bera, S. C.; Maiti, S.; Chattopadhyay, N. *Biophys. Chem*. **2004**, *112*, 9.
(22) Stolc, S. *Life. Sci*. **1999**, *65*, 1943.
(23) Dias, A.; Varela, A. P.; Miguel, M. G.; Macanita, A. L.; Becker, R. S.; Burrows, H. D. *J. Phys. Chem*. **1996**, *100*, 17970.
(24) Varela, A. P.; Miguel, M. G.; Macanita, A. L.; Becker, R. S.; Burrows, H. D. *J. Phys. Chem.* **1995**, *99*, 16093.
(25) Mallick, A.; Chattopadhyay, N. *Photochem. Photobiol*. **2005**, *81*, 419.
(26) Mallick, A.; Haldar, B.; Chattopadhyay, N. *J. Photochem. Photobiol., B* **2005**, *78*, 215.
(27) Chattopadhyay, N.; Dutta, R.; Chowdhury, M. *J. Photochem. Photobiol., A* **1989**, *47*, 249.
(28) Giri, V. S.; Maiti, B. C.; Pakrashi, S. C. *Heterocycles* **1984**, *22*, 233.
(29) Sarkar, N.; Das, K.; Datta, A.; Das, S.; Bhattacharya, K. *J. Phys. Chem*. **1996**, *100*, 10523.
(30) Demas, J. N.; Crosby, G. A. *J. Phys. Chem*. **1971**, *75*, 991.
(31) Mallick, A.; Maiti, S.; Haldar, B.; Purkayastha, P.; Chattopadhyay, N. *Chem. Phys. Lett.* **2003**, *371*, 688.
(32) Wang, M.; Thomas, J. K.; Gratzel, M. *J. Am. Chem. Soc*. **1976**, *98*, 2391.
(33) Guharay, J.; Sengupta, P. K. *Chem. Phys. Lett*. **1994**, *75*, 230.
(34) Kelker, Devaki A.; Chattopadhyay, A. *J. Phys. Chem. B* **2004**, *108*, 12151.
(35) Mukherjee, S.; Chattopadhyay, A. *J. Fluoresc.* **1995**, *5*, 237.
(36) Lakowicz, J. R. *Principles of Fluorescence Spectroscopy*; Plenum: New York, 1983.
(37) Sarkar, N.; Das, K.; Datta, A.; Das, S.; Bhattacharya, K. *J. Phys. Chem. B* **1996**, *100*, 10523.
(38) Hof, M.; Lianos, P.; Laschewsky, A. *Langmuir* **1997**, *13*, 2181.
(39) Sarkar, M.; Ray, J. G.; Sengupta, P. K. *J. Photochem. Photobiol., A* **1996**, *95*, 157.
(40) Sengupta, B.; Sengupta, P. K. *Biochem. Biophys. Res. Commun*. **2000**, *277*, 13.
(41) Bismuto, E.; Jameson, D.; Gratton, M. E. *J. Am. Chem. Soc*. **1987**, *109*, 5414.
(42) Kossower, E. M.; Kantey, H. *J. Am Chem. Soc*. **1983**, *105*, 6236.
(43) Macgregor, R. B.; Weber, G. *Nature* **1986**, *319*, 70.
(44) Ghosh, S. K.; Bhattacharya, S. C. *Chem. Phys. Lipids* **2004**, *131*, 151.
(45) Dennison, S. M.; Guharay, J.; Sengupta, P. K. *Spectrochim. Acta, Part A* **1999**, *55*, 1127.
(46) Reichardt, C. In *Molecular Interaction*, Vol. 3; Ratajazak, H., Orville-Thomas, W. J., Eds.; Wiley: New York, 1982; p 255.
(47) Kossower, E. M.; Doudik, H.; Tanizawa, K.; Ottolenghi, M.; Orbach, N. *J. Am. Chem. Soc*. **1975**, *97*, 2167.
(48) Wang, X.; Wang, J.; Wang, Y.; Yan, H.; Li, P.; Thomas, R. K. *Langmuir* **2004**, *20*, 53.
(49) Hanegawa, M.; Sugimura, T.; Suzani, Y.; Shindo, Y.; Kitahava, A. *J. Phys, Chem.* **1994**, *98*, 2120.
(50) Lide, D. R., Ed. *Handbook of Chemistry and Physics*, 78th ed.; CRC Press: Boca Raton, FL, 1997.
(51) Andrade, S. M.; Costa, S. M. B.; Pansu, R. *Photochem. Photobiol.* **2000**, *71*, 485.
(52) Raghuraman, H.; Pradhan, S. K.; Chattopadhyay, A. *J. Phys. Chem. B* **2004**, *108*, 2489.
(53) Panda, M.; Behera, P. K.; Misra, B. K.; Behera, G. B. *J. Photochem. Photobiol., A* **1995**, *90*, 69.
(54) Moran, M.; Bowmaker, G. A.; Cooney, R. P. *Langmuir* **1995**, *11*, 738.
(55) Eastoe, J.; Towey, T. F.; Robinson, B. H.; Williams, J.; Heenan, R. K. *J. Phys. Chem.* **1993**, *97*, 1459.
(56) Prendergast, F. G. *Curr. Opin. Struct. Biol*. **1991**, *1*, 1054.
(57) Chattopadhyay, A.; Mukherjee, S.; Raghuraman, H. *J. Phys. Chem. B* **2002**, *96*, 7919.
(58) Torphin, D.; Svodova, J.; Konopasek, I.; Brand, L. J. *J. Chem. Phys.* **1992**, *96*, 7919.
(59) Chattopadhyay, A.; Mukherjee, S.; Raghuraman, H. *J. Phys. Chem. B* **2002**, *106*, 13002.
(60) Datta, A.; Mandal, D.; Pal, S. K.; Bhattacharya, K. *J. Phys. Chem. B* **1997**, *101*, 10221.

(61) Chattopadhyay, N.; Serpa, C.; Pereira, M. M.; Seixas de Melo, J.; Arnaut, L. G.; Formoshino, S. J. *J. Phys. Chem. A* **2001**, *105*, 10025.
(62) Kossower, E. M. *Acc. Chem. Res*. **1982**, *15*, 259.
(63) Kossower, E. M.; Doudik, H. *J. Phys. Chem.* **1978**, *82*, 2012.
(64) Weber, G.; Haris, F. G. *Biochemistry* **1979**, *18*, 3075.
(65) Kossower, E. M.; Tanizawa, K. *Chem. Phys. Lett*. **1972**, *16*, 419.
(66) Hicks, J. M.; Vandershall, M. T.; Sitzmann, E. V.; Eisenthal, K. B. *Chem. Phys. Lett.* **1987**, *135*, 18.
(67) Hicks, J. M.; Vandershall, M. T.; Sitzmann, E. V.; Eisenthal, K. B. *Chem. Phys. Lett.* **1987**, *135*, 413.